Microtacticity Distribution of Polypropylenes Prepared with Heterogeneous Ziegler-Natta Catalysts

Masahiro Kakugo,* Tatsuya Miyatake, Yukio Naito, and Kooji Mizunuma

Chiba Research Laboratory, Sumitomo Chemical Co., Ltd., 5-1 Anesakikaigan, Ichihara, Chiba 299-01, Japan. *Received January 27, 1987*

ABSTRACT: The microstructure of the isotactic parts of various polypropylenes has been studied by ^{13}C NMR spectroscopy. The isotacticity of the isotactic parts as determined by the *mmmm* pentad sequence ("microisotacticity") increases as the stereospecificity of the catalysts (isotactic index, II) employed increases. Several polypropylenes prepared with titanium-based catalysts were fractionated by using an elution column technique. The fractionation results show that two isospecific active centers reside in such catalysts. The proportion of those active centers varies with catalyst; the highly isospecific center increases with the stereospecificity (II). This fact accounts for the above relationship between the microisotacticity and the stereospecificity. On the basis of these results, new models for the active centers are proposed.

Introduction

It is well-known that heterogeneous Ziegler-Natta catalysts yield a mixture of polypropylenes having different stereoregularities, i.e., isotactic and atactic. From the industrial point of view, the formation of atactic polymer is a key concern because it has a great influence on the production cost and the physical properties of the products. Thus, efforts have been directed toward the reduction of atactic polymer. On the other hand, it is the isotactic polymer that is the major component of commercial polypropylenes. For example, the isotactic index (II) of commercial polypropylenes (i.e., boiling heptane insoluble fraction) generally exceeds 95%. Therefore, the molecular microstructure of an isotactic polymer probably has a significant influence on the properties of the products. Although the microtacticity of the isotactic parts is known to vary subtly with catalyst system,[1-5] no detailed studies have so far been carried out. The objective of the present paper is specifically to understand the relationship between the nature of catalysts and the molecular structure of the isotactic parts. First, the isotactic fractions of polypropylenes polymerized with a wide range of heterogeneous catalysts have been examined by ^{13}C NMR spectroscopy. Next, a microtacticity distribution of several polypropylenes has been determined by temperature-programmed column fractionation. As a result, it has been found that: (1) two isospecific active centers are present and (2) the relative proportion of the active centers varies with catalyst. These results will be discussed on the basis of the newly proposed models for the active centers.

Experimental Section

Catalysts. δ-$TiCl_3$HA, δ-$TiCl_3$AA, δ-$TiCl_3$ (Solvay), $CrCl_3$, and VCl_3 were purchased and were used without any treatment except that $CrCl_3$ was ball-milled for the purpose of improvement of its catalytic activity. δ-$TiCl_3$HA was obtained from Toyo Stauffer Chemical and had been prepared by reduction of $TiCl_4$ with hydrogen, followed by ball-milling. δ-$TiCl_3$AA which had been prepared by reduction of $TiCl_4$ with aluminum followed by ball-milling for activation was also obtained from Toyo Stauffer Chemical. δ-$TiCl_3$ (Solvay) was obtained from Solvay-Marubeni Chemicals Co. β-$TiCl_3$ was prepared from the Natta complex according to Smith and Perry.[6] $MgCl_2$-supported Ti catalyst was prepared according to the Sumitomo Chemical Co. patent.[7] Ethylaluminum (EtAl) cocatalysts and methyl *p*-toluate as an electron donor were purchased and were used without any purification.

Polymerization. Polymerization was carried out in a 5-L autoclave in liquefied propylene or in *n*-heptane, both of which were dried on a molecular sieve 13× in advance. The polymerization was terminated by adding isobutyl alcohol. After the catalyst residues were removed with a mixture of 1 N HCl and methanol (1/1 v/v), the product was dried in vacuo at 50 °C for 4 h. Detailed polymerization conditions are given in Tables I and II. The aging of δ-$TiCl_3$AA was carried out at 70 °C similarly to the polymerization except that there was no feed of the monomer; after 3.5 h the polymerization was initiated by introducing the monomer.

Solvent Extraction. The sample was completely dissolved in boiling xylene and then the solution was cooled gradually to 20 °C. The precipitated polymer was separated from the solution by filtration. The polymer soluble in xylene at 20 °C was recovered from the filtrate by evaporation. Further, the precipitated polymer was extracted with boiling *n*-heptane in a Soxhlet extractor.

Elution Column Fractionation. Ten grams of the whole polymer was dissolved at 130 °C in xylene, and then 1200 g of sea sand (35-48 mesh) kept at 130 °C was put into the solution. The mixture was cooled gradually to 20 °C. Through this treatment, the higher isotactic polymer will be deposited first and the lower last, which will achieve a satisfactory fractionation. Then the mixture was put into a column (74 mm in diameter and 435 mm in height) immersed in an oil bath maintained at 20 °C. The first fractionation was eluted at 20 °C by dropping xylene into the column. Five hundred milliliters of xylene was used to elute each fraction. However, when a precipitate or milky turbidity appeared by addition of last several droplets of the eluate into methanol, some additional xylene was introduced until it did not appear. The time taken was about 1 h. The consecutive fractions were obtained by raising the elution temperature stepwise up to 130 °C. The polymer fractions were precipitated by addition of the eluates by into 2.5 L of methanol, recovered by filtration, and dried in vacuo. The fractions were obtained every 10 to 20 °C in the region 20-60 °C, every 2 to 10 °C in the region 60-90 °C, every 1 to 2 °C in the region 90-110 °C, and every 0.5 to 1 °C at over 110 °C. The elution temperature was controlled within ±0.1 °C. As a result, the number of the fractions varies from 16 to 38, depending on the isotacticity of the samples. The differential distribution was determined from slope of the cumulative distribution.

^{13}C NMR Measurement. ^{13}C NMR spectrum was obtained at 135 °C on a JEOL FX-100 pulsed Fourier transform NMR spectrometer. Experimental procedure and instrument conditions are described in a previous paper.[8] Pentad tacticity was determined from the area of the resonance peaks of the methyl region. Pentad sequences are represented by a sequence of *m* = meso (isotactic diads) and *r* = racemic (syndiotactic diads).

Melting Temperature Measurement. The melting temperature of the sample was measured on a Perkin-Elmer type-2 differential scanning calorimeter (DSC). The sample was premelted in DSC at 220 °C for 5 min and was rapidly cooled to room temperature. The thermogram was recorded by raising the temperature from 40 to 180 °C at a rate of 5 °C/min.

Results

Extraction of Polypropylenes Polymerized with Various Catalyst Systems. A variety of polypropylenes prepared with transition-metal halides such as $TiCl_3$, VCl_3,

0024-9297/88/2221-0314$01.50/0

Table I
Stereoregularity of Polypropylenes Prepared with Various Catalysts Systems

		polymerization[a]			solvent extraction		
sample	catalyst system	temp, °C	time, h	catal act, g of PP/(g of cat h)	atactic,[b] %	isotactic,[c] %	microisotacticity[d]
1	δ-$TiCl_3$AA–$AlEt_2Cl$	60	1	400	5.00	90.2	0.967
2	δ-$TiCl_3$Sol[e]–$AlEt_2Cl$	60	1	2000	3.0	92.2	0.973
3	δ-$TiCl_3$HA–$AlEt_2Cl$	65	4	120	10.7	82.9	0.962
4	β-$TiCl_3$–$AlEt_2Cl$	65	4	140	62.6	18.7	0.956
5	VCl_3–$AlEt_2Cl$	65	4	50	55.1	14.3	0.956
6	$CrCl_3$–$AlEt_2Cl$	65	4	1	18.4	71.7	0.960
7	δ-$TiCl_3$AA–$AlEt_3$	60	1	710	14.9	60.0	0.964
8	δ-$TiCl_3$AA–$AlEt_2Br$	60	1	530	6.0	88.4	0.965
9	δ-$TiCl_3$AA–$AlEt_2I$	60	1	200	2.9	92.9	0.975
10	δ-$TiCl_3$SOL–$AlEt_3$	70	1	5600	23.3	59.1	0.958
11	δ-$TiCl_3$SOL–$AlEt_2I$	50	1	600	1.0	95.4	0.983

[a] Other polymerization conditions: 5-L autoclave; propylene, 33 mol; H_2, 2–5 vol %; $AlEt_2Cl$, 25 mmol; $AlEt_3$, 4 mmol; $AlEt_2Br$, 25 mmol; $AlEt_2I$, 25 mmol. [b] % fraction soluble in xylene at 20 °C. [c] % fraction insoluble in boiling *n*-heptane. [d] [*mmmm*] fraction of the fraction insoluble in boiling *n*-heptane. [e] δ-$TiCl_3$ (Solvay).

Table II
Sample List for Fractionation

		polymerization[a]					solvent extraction		
sample	catalyst system	time, h	pressure, kg/(cm G)	H_2, vol %	catal act, g of PP/(g of cat h)	IV,[b] dL/g	atactic,[c] %	isotactic,[c] %	microisotacticity
12	β-$TiCl_3$–$AlEt_2Cl$	0.5	10	1.5	80	0.6	62.7		0.955
13	δ-$TiCl_3$AA–$AlEt_2Cl$	0.5	10	5.1	640	1.6	5.1		0.967
14	δ-$TiCl_3$AA–$AlEt_2Cl$	0.5[d]	10	3.7	420	1.5	6.2		0.964
15	Mg–Ti(I)[e]–$AlEt_3$	1.0	6	2.8	8900	0.7	43.0	28.0	0.954
16	Mg–Ti(I)[e]–$AlEt_3$–MT[f]	1.0	6	2.8	5400	1.8	4.7	88.4	0.970

[a] Other polymerization conditions: 5-L autoclave; solvent *n*-heptane, 1.5 L; polymerization temperature, 70 sC; $AlEt_2Cl$ 12.5 mmol; $AlEt_3$, 4.0 mmol; MT, 0.88 mmol. [b] Intrinsic viscosity. [c] See Table I. [d] The catalyst was aged for 3.5 h at 70 °C in advance of polymerization. [e] According to U.S. Patent 4 223 117 (Sumitomo Chemical Co.). [f] Methyl *p*-toluate.

and $CrCl_3$ and $MgCl_2$-supported Ti catalysts with and without methyl *p*-toluate as an electron donor were divided into three fractions, those soluble in xylene at 20 °C, soluble in boiling heptane, and insoluble in boiling heptane, by conventional solvent extraction method. The stereoregularity of the fractions insoluble in boiling heptane was determined by ^{13}C NMR spectroscopy. The extraction data are shown in Tables I and II. As seen from these tables, the percent of atactic polymer (soluble in xylene at 20 °C) varies over a wide range of 1–63% and at the same time the II ranges from 14 to 95%. In addition, the isotactic (*mmmm*) pentad fraction of the isotactic parts as measured by ^{13}C NMR also varies ranging from 0.956 to 0.983. The isotactic pentad fraction will hereinafter be termed "microisotacticity" in order to be distinguished from the so-called isotactic index, II. Similarly the ability to regulate the microisotacticity will be termed "microisospecificity".

Strangely, the data shown in Tables I and II suggest that the variation of microisotacticity may have some relation to that of percent atactic polymer. As noted in Figure 1, the microisotacticity shows a tendency to decrease with increasing percent atactic polymer. Although a $MgCl_2$-supported Ti catalyst is not highly stereospecific in the absence of an electron donor, it is of interest that the microisotacticity also decreases in its absence. The pentad stereoirregularities found in all the isotactic parts are only *mmmr*, *mmrr*, and *mrrm*. The ratio of those intensities is approximately 2:2:1. This fact indicates that isotactic propagation on all the catalysts used here is governed by catalytic control,[1,10] which means that the nature of the isotactic active center determines the microisotacticity. On the other hand, the percent atactic polymer is presumed to reflect only the relative concentration of the atactic active center. Therefore, it is rather unusual that the microisospecificty of the isotactic active center is directly

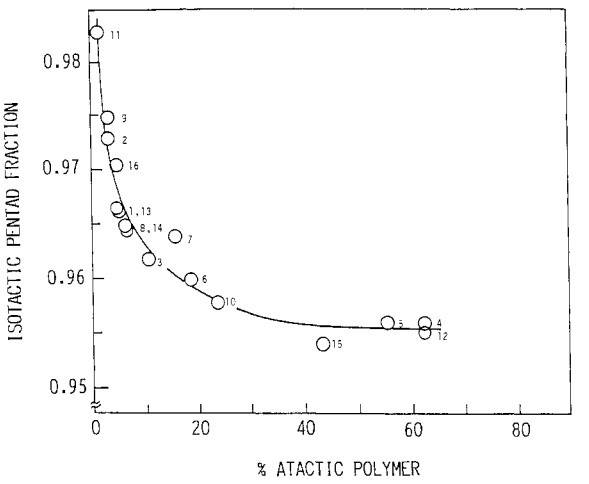

Figure 1. Plot of microisotacticity against percent atactic polymer. Catalyst systems: (1) δ-$TiCl_3$AA–$AlEt_2Cl$; (2) δ-$TiCl_3$SOL–$AlEt_2Cl$; (3) δ-$TiCl_3$HA–$AlEt_2Cl$; (4) β-$TiCl_3$–$AlEt_2Cl$; (5) VCl_3–$AlEt_2Cl$; (6) $CrCl_3$–$AlEt_2Cl$; (7) δ-$TiCl_3$AA–$AlEt_3$; (8) δ-$TiCl_3$AA–$AlEt_2Br$; (9) δ-$TiCl_3$AA–$AlEt_2I$; (10) δ-$TiCl_3$SOL–$AlEt_3$; (11) δ-$TiCl_3$SOL–$AlEt_2I$; (12) β-$TiCl_3$–$AlEt_2Cl$; (13) δ-$TiCl_3$AA–$AlEt_2Cl$; (14) δ-$TiCl_3$AA–$AlEt_2Cl$; (15) $MgCl_2$-supported Ti–$AlEt_3$; (16) $MgCl_2$-supported Ti–$AlEt_3$–methyl *p*-toluate.

correlated with the concentration of the atactic active center. In order to understand this correlation, we have investigated a detailed microtacticity distribution. The samples listed in Table II were fractionated by a temperature-programmed elution column technique.

Microtacticity Distribution of the Polypropylenes Polymerized with the β- and δ-$TiCl_3$ Catalysts. As seen from Tables I and II, β-$TiCl_3$–$AlEt_2Cl$ (samples 4 and 12) shows very low stereospecificity (percent atactic polymer; 63%), while δ-$TiCl_3$–$AlEt_2Cl$ (samples 1, 2, 3, and 13) shows high stereospecificity (percent atactic polymer; <11%).

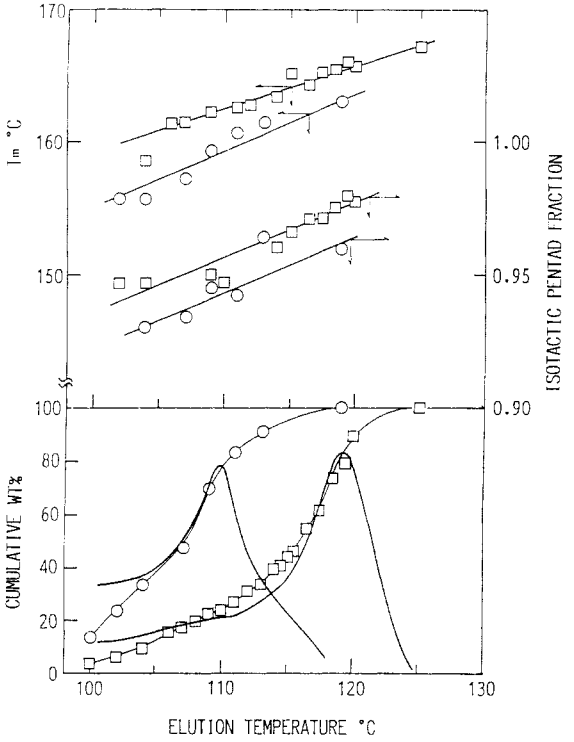

Figure 2. Cumulative and differential fractionation curves and the melting temperatures and the isotactic pentads (*mmmm*) of the fractions. Catalyst systems: (○) β-$TiCl_3$–$AlEt_2Cl$ (sample 12); (□) δ-$TiCl_3AA$–$AlEt_2Cl$ (sample 13).

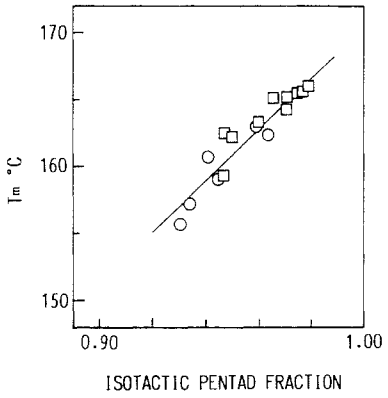

Figure 3. Relationships between the melting temperature (T_m) and the isotactic pentad fraction. Catalyst systems: (○) β-$TiCl_3$–$AlEt_2Cl$ (sample 12); (□) δ-$TiCl_3AA$–$AlEt_2Cl$ (sample 13).

Furthermore, both catalysts significantly differ from each other in microisospecificity. Thus, the following studies were undertaken to determine the relationship between catalyst structure and the microisotacticity. The cumulative and differential distribution curves in the region of over 100 °C are illustrated in Figure 2, where the melting temperatures and isotactic pentad fractions for the individual fractions are also plotted, both increasing linearly with an increase in elution temperature. These data indicate that the fractionation takes place according to isotacticity as would be expected. The fractionation data clearly show that the polymer (sample 12) prepared with the β-$TiCl_3$ catalyst is a low isotactic polymer compared with that (sample 13) prepared with the δ-$TiCl_3$ catalyst. Next the isotactic pentad fractions of both polymers are plotted against the melting temperatures in Figure 3, where a straight line is given irrespective of a significant difference in molecular weight, 2.5×10^5 for the polymer prepared with the β-$TiCl_3$ catalyst and 3.2×10^5 for that prepared with the δ-$TiCl_3$ catalyst. Accordingly, the isotactic pentad fraction can be determined from the melting temperature. Subsequently the isotactic pentad fraction was determined from the melting temperature by using this relationship.

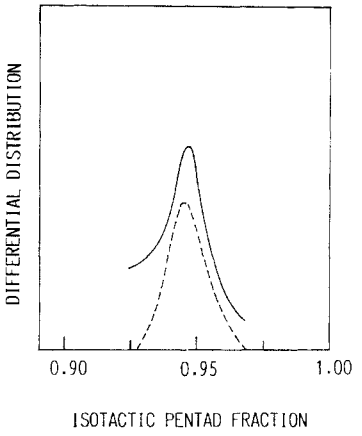

Figure 4. Microtacticity distribution curves. Catalyst system β-$TiCl_3$–$AlEt_2Cl$ (sample 12): (—) observed curve; (- - -) calculated curve ([*mmmm*] = 0.945, M_n = 252 000).

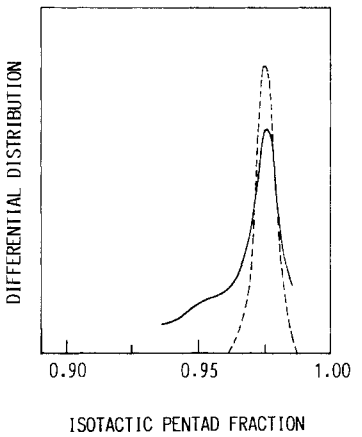

Figure 5. Microtacticity distribution curves. Catalyst system δ-$TiCl_3AA$–$AlEt_2Cl$ (sample 13): (—) observed curve; (- - -) calculated curve ([*mmmm*] = 0.975, M_n = 315 000).

The stereoregularity of isotactic polypropylene can be expressed by the enantiomorphous model,[1] and therefore, a microtacticity distribution can be calculated on the basis of a binominal distribution. The calculated and observed curves are shown in a differential distribution form in Figures 4 and 5 for the β- and δ-$TiCl_3$ catalysts. Since extremely precise fractionations were achieved, the observed differential curves are believed to be highly reliable. One can see an excellent agreement between the calculated and observed curves in the β-$TiCl_3$ catalyst. This result strongly suggests that the β-$TiCl_3$ catalyst contains only a single isospecific center. On the other hand, two polymers different in microtacticity are observed in the δ-$TiCl_3$ catalyst system: a predominant peak at the isotactic pentad of 0.975 and a discernible shoulder at the region of the isotactic pentad of ca. 0.95. The predominant peak agrees closely with the distribution calculated on the basis of a single active center. However, the shoulder appears to result from another active center. This result suggests that at least two isospecific centers differing in microisospecificity are present in the δ-$TiCl_3$ catalyst.

As shown in Figure 6, the δ-$TiCl_3$ catalyst produces polypropylene with increasingly lower II with the extent of polymerization. At the same time, the microisotacticity also decreases as can be seen from a decrease in the melting temperature. Such change may be explained if the higher isospecific active center decays predominantly. If the

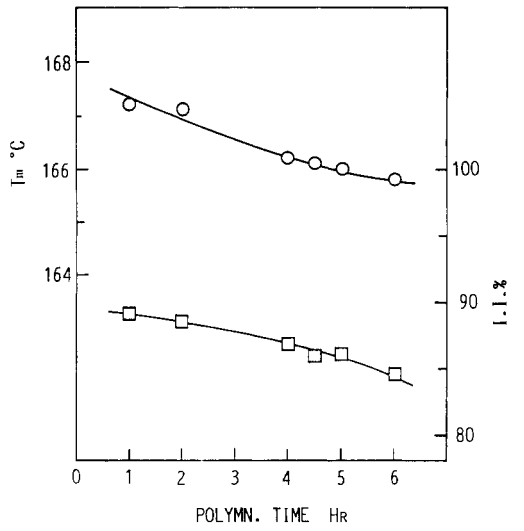

Figure 6. Decrease in the melting temperature (T_m) and the percent II of the polymer with the proceeding of polymerization, catalyst system δ-$TiCl_3AA$–$AlEt_2Cl$. Polymerization conditions: 5-L autoclave; propylene 33 mol; H_2 4 vol %; $AlEt_2Cl$ 25 mmol; (○) melting temperature (T_m); (□) percent II.

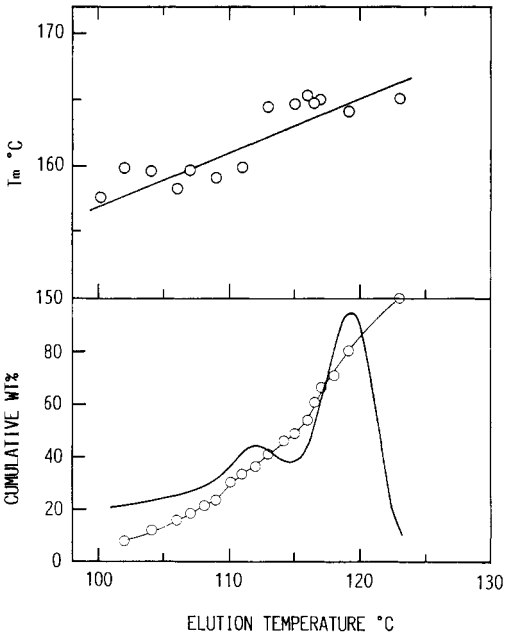

Figure 7. Cumulative and differential fractionation curves and melting temperature (T_m) of the fractions; catalyst system δ-$TiCl_3AA$–$AlEt_2Cl$, after aging (sample 14).

assumption is accepted, the low microisotactic polymer should increase in a polymer prepared with an aged catalyst relative to the age of the catalyst. Accordingly, we have examined the polymer (sample 14) polymerized with the δ-$TiCl_3$ catalyst aged for 3.5 h at polymerization temperature (70 °C). As shown in Table II, the aging reduces the polymerization rate. The fractionation results are illustrated in Figure 7, where one can see that the low microisotactic peak is increased relative to the age of the catalyst. This experimental result highly supports the presence of two isospecific active centers. In addition, the decay behavior indicates that they are likely to be chemically different from each other. The microtacticity distribution calculated on the basis of two active centers is shown in Figure 8 together with the observed one. Excellent agreement can be seen between them.

Microtacticity Distribution of the Polypropylenes Polymerized with the $MgCl_2$-Supported Ti Catalyst

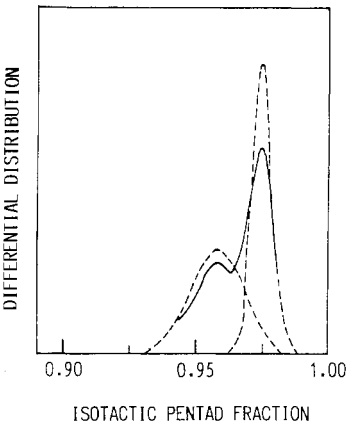

Figure 8. Microtacticity distribution curves. Catalyst system δ-$TiCl_3AA$–$AlEt_2Cl$ after aging (sample 14): (—) observed curve; (- - -) calculated curves ([*mmmm*] = 0.958, M_n = 84 000 and [*mmmm*] = 0.975, M_n = 315 000).

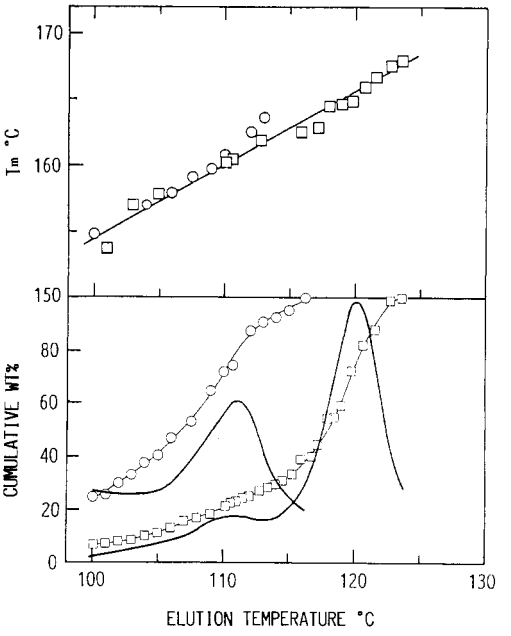

Figure 9. Cumulative and differential fractionation curves, and the melting temperature (T_m) of the fractions: (○) $MgCl_2$-supported Ti–$AlEt_3$ (sample 15); (□) $MgCl_2$-supported Ti–$AlEt_3$–methyl *p*-toluate (sample 16).

System. The polymers prepared with the $MgCl_2$-supported Ti catalyst systems have been examined in a similar manner. Figure 9 shows the cumulative and differential distribution curves together with the melting temperatures for the polymers polymerized by the $MgCl_2$-supported Ti catalyst with and without methyl *p*-toluate as an electron donor (samples 15 and 16). In the absence of the electron donor, a single peak is seen at the elution temperature of 111 °C. This elution temperature is close to that of the peak in the β-$TiCl_3$. On the other hand, in the presence of the electron donor, two peaks are seen: a main peak at 121 °C and a small peak at 111 °C. The latter peak is located very close to the peak observed when the electron donor was not added. Figure 10 shows comparisons between the observed and calculated distribution curves for polymers both with and without methyl *p*-toluate. In each case excellent agreement is found between the observed and the calculated curves.

The conclusion to be drawn from these experimental results is as follows. Only a low isospecific center resides in the low stereospecific catalysts such as the β-$TiCl_3$ catalyst and the $MgCl_2$-supported Ti catalyst without

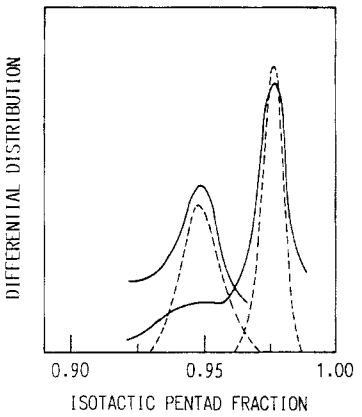

Figure 10. Microtacticity distribution curves. Catalyst system $MgCl_2$-supported Ti: (—) observed curves; (---) calculated curves ([*mmmm*] = 0.949, M_n = 200 000 and [*mmmm*] = 0.976, M_n = 386 000).

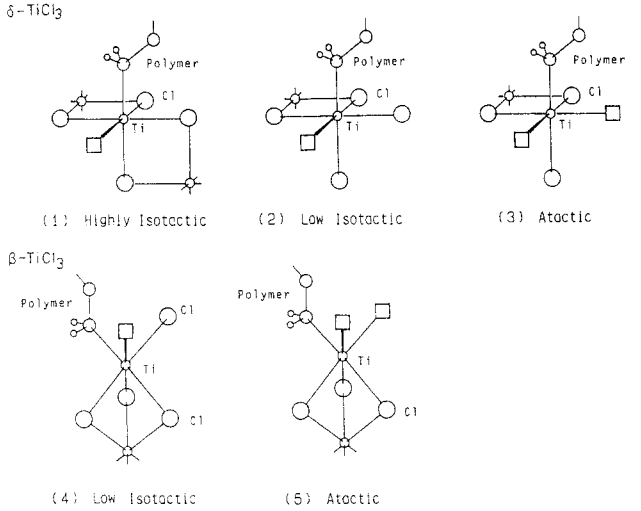

Figure 11. Models for the active centers on β- and δ-$TiCl_3$; (□) Cl vacancy.

electron donor. On the other hand, highly stereospecific catalysts such as the δ-$TiCl_3$ catalyst and the $MgCl_2$-supported Ti catalyst containing the electron donor bear predominantly the highly isospecific center and a small portion of the low isospecific center. The relationship shown in Figure 1 could be accounted for in terms of the variation of the proportion of these centers.

Discussion

As described above, β-$TiCl_3$ and δ-$TiCl_3$ significantly differ from each other in both isospecificity and microisospecificity. Such a large difference is presumed primarily to result from a difference in crystal structure. Fortunately, their crystalline structure is well characterized. β-$TiCl_3$ has a linear (chain like) structure, while δ-$TiCl_3$ has a layered structure.[9] According to Arlman and Cossee,[11,12] the isospecific active center in the δ-$TiCl_3$ consists of four firmly bound Cl ions, an alkyl group, and a Cl vacancy (model 1) as shown in Figure 11. On the other hand, β-$TiCl_3$ consists of the chainlike unit. The isospecific center in the β-$TiCl_3$, therefore, may consist of three firmly bound Cl ions, a loosely bound Cl ion, a Cl vacancy, and an alkyl group bound to the Ti atom of the chain end (model 4). From a comparison between two models, the former active center appears to be structurally more rigid than the latter active center because the Cl ions are all bound to Ti atoms. The former active center may therefore possess stronger microisospecificity. The lower isospecific center (isotactic pentad; 0.96) seen in the δ-$TiCl_3$ is close to the isospecific center (isotactic pentad; 0.95) in β-$TiCl_3$ with respect to microisospecificity. The active center, containing a loosely bound Cl ion (model 2) may be attributed to the low isospecific center by analogy with model 4 for β-$TiCl_3$. The active centers having two vacancies (models 3 and 5) probably become nonstereospecific centers.

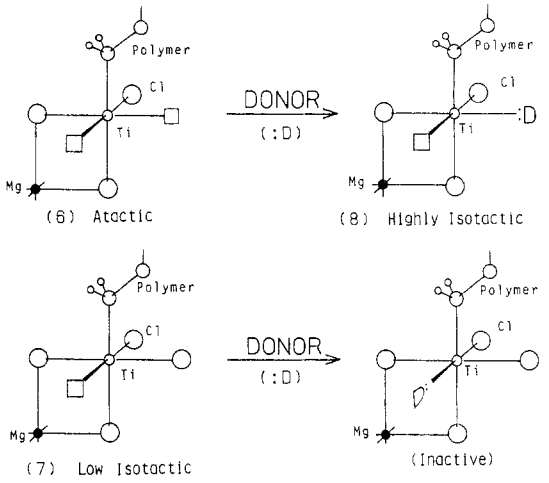

Figure 12. Models for the active centers on supported Ti catalyst and the effect of an electron donor; (□) Cl vacancy.

Judging from the preparation method, the $MgCl_2$-supported Ti catalysts are considered to possess two types of active centers as follows.

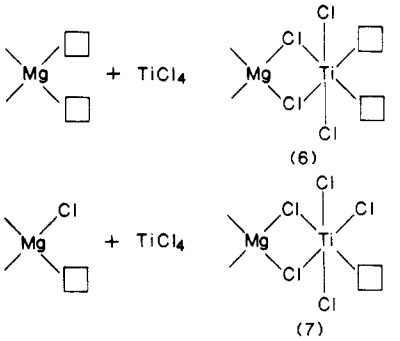

By analogy with β-$TiCl_3$ it seems reasonable that the active center containing two Cl vacancies (model 6) is nonstereospecific and that containing loosely bounded Cl's and a Cl vacancy (model 7) is low isospecific. As shown in Figure 12, the addition of the electron donor may convert the nonstereospecific center to the high isospecific one (model 8), and the low isospecific center to an inactive one.

Registry No. MT, 99-75-2; $TiCl_3$, 10025-73-7; VCl_3, 7705-07-9; $CrCl_3$, 7718-98-1; $AlEt_2Cl$, 96-10-6; $AlEt_3$, 97-93-8; $AlEt_2Br$, 760-19-0; $AlEt_2I$, 2040-00-8; $MgCl_2$, 7786-30-3; isotactic polypropylene, 25085-53-4.

Supplementary Material Available: Tables of raw fractionation data on five samples (5 pages). Ordering information is given on any current masthead page.

References and Notes

(1) Wolfsgruber, C.; Zannoni, G.; Rigamonti, E.; Zambelli, A. *Makromol. Chem.* **1975**, *176*, 2765.
(2) Bukatov, G. D.; Zakharov, V. A.; Yermakov, Y. I. *Makromol. Chem.* **1978**, *179*, 2093.
(3) Doi, Y.; Suzuki, E.; Keii, T. *Makromol. Chem., Rapid Commun.* **1981**, *2*, 293.
(4) Doi, Y.; Keii, T. *Makromol. Chem.* **1978**, *179*, 2117.
(5) Rishina, L. A.; Kissin, Yu, V.; Dyachkovsky, F. S. *Eur. Polym. J.* **1976**, *12*, 727.
(6) Smith, G. H.; Perry, D. C. *J. Polym. Sci., Polym. Chem. Ed.* **1969**, *7*, 707.
(7) Sumitomo Chemical Co., U.S. Patent 4 223 117, Sept 16, 1980.

(8) Kakugo, M.; Naito, Y.; Mizunuma, K.; Miyatake, T. *Macromolecules* **1982**, *15*, 1150.
(9) Natta, G.; Corradini, P.; Allegra, G. *J. Polym. Sci.* **1961**, *51*, 399.
(10) Shelden, R. A.; Fueno, T.; Tsunetsugu, T.; Furukawa, J. *J. Polym. Sci., Part B* **1965**, *3*, 23.
(11) Arlman, E. J.; Cossee, P. *J. Catal.* **1964**, *3*, 99.
(12) Arlman, E. J. *J. Catal.* **1966**, *5*, 178.

Polymerization of Diene-Containing Lipids as Liposomes by Radical Initiators. 4.[1] Effect of Lipid Packing on the Polymerization Profile

Hiroyuki Ohno, Shinji Takeoka, Hidetaka Iwai, and Eishun Tsuchida*

Department of Polymer Chemistry, Waseda University, Tokyo 160, Japan.
Received April 23, 1987

ABSTRACT: 1,2-Di(2,4-octadecadienoyl)-*sn*-glycero-3-phosphorylcholine (DODPC) was polymerized as liposomes with a water-soluble radical initiator, azobis(2-amidinopropane) dihydrochloride (AAPD). DODPC liposomes were prepared with a tip-type sonicator and incubated at 4, 8, or 20 °C. When DODPC liposomes were incubated at lower temperatures than the gel-to-liquid crystalline phase transition temperature (16 °C for DODPC liposomes), these liposomes fused with each other to produce large unilamellar liposomes. An average radius was calculated from the ^{1}H NMR signal intensity ratio for the choline methyl protons split by Eu^{3+}. Generally AAPD initiated radical polymerization of diene groups on the 2-acyl chains of DODPC because of nonequivalent acyl chain packing in bilayer membranes. The polymerization conversion for larger DODPC liposomes reached about 50% by AAPD-initiated polymerization. An excess polymerization was initiated by AAPD when liposomes were not incubated unless the average radius was smaller than 30 nm. This is explained by the disordered lipid packing for small liposomes. This disordered lipid packing permits invasion of water molecules deeper into the hydrophobic region of the outer half of the bilayer membrane of the liposomes, attributed to a larger curvature. For small DODPC liposomes the AAPD radicals could therefore reach diene groups in even 1-acyl chains which were essentially not attacked by AAPD radicals from an aqueous phase as long as lipids were well oriented. The increase of polymerization conversion may be due to an entropically semistable lipid packing inevitable for smaller liposomes. It is concluded that the well-defined selective polymerization of diene groups in 2-acyl chains of DODPC lipids requires liposomes larger in size than with a 30-nm radius.

Introduction

Phospholipid bilayer liposomes are widely applied as microcapsules for drugs or functional molecules as well as models for biomembranes. These liposomes, however, are generally not stable and undergo aggregation and fusion. To stabilize these assembled structures, polymerizable amphiphiles have been incorporated as a major component to construct stable membrane structures by polymerization. In our previous papers, unilamellar liposomes composed of 1,2-di(2,4-octadecadienoyl)-*sn*-glycero-3-phosphorylcholine (DODPC), which contained diene groups in both acyl chains were polymerized by radical initiators.[2,3] Either water-insoluble azobis(isobutyronitrile) (AIBN) or water-soluble azobis(2-amidinopropane) dihydrochloride (AAPD) provided polymerization conversion of around 50% for this lipid. A simultaneous polymerization by these radical initiators resulted in complete polymerization, and the resulting polymerized DODPC liposomes showed excellent stability against physical or chemical stimuli such as sonication or detergent attack.[3] However, this monomeric lipid had polymerizable diene groups in the same position (2,4-diene) in two acyl chains, and it appeared very likely that these acyl chains showed nonequivalent reactivities against water-soluble or -insoluble radical initiators.[3] Polymerization of diene groups bound to the 1-acyl chains was initiated by the addition of AIBN. On the other hand, the diene groups on the 2-acyl chains were believed to face an aqueous phase and were polymerized by the addition of water-soluble radical initiators. This was confirmed by the same polymerization experiments with a monodiene-type polymerizable lipid, 1-palmitoyl-2-(2,4-octadecadienoyl)-*sn*-glycero-3-phosphorylcholine which possessed one diene group only in the 2-acyl chain. It was clearly demonstrated that the polymerization of diene groups in the 2-acyl chains was initiated only by water-soluble radical initiators.[4] All of the results strongly support the possibility of a selective polymerization of polymerizable amphiphiles in an assembled structure. This selective polymerization, however, was not so clear for very small DODPC liposomes. This suggested that the radical polymerization of these systems should be affected by the lipid packing in the liposomes. This study was therefore intended to elucidate the effect of lipid packing in liposomes on their polymerization profiles.

Experimental Section

Materials. 1,2-Di(2,4-octadecadienoyl)-*sn*-glycero-3-phosphorylcholine (DODPC) was purchased form Nippon Oil & Fats Co., Ltd. This was characterized by thin-layer chromatography (Merck, silica gel plates) with chloroform/methanol/water (65/35/5, by vol) as eluant before use.[3] A polymerizable lipid which showed a single spot on the TLC plate was used without purification. Azobis(2-amidinopropane) dihydrochloride (AAPD) was purchased from Tokyo Kasei Co. Ltd. and was purified by recrystallization twice from water.

Methods. A total of 0.200 g of lipids was dissolved in dry chloroform and was slowly evaporated in a rotating sample tube to prepare a thin lipid film on the inner surface of the tube. Twenty milliliters of degassed distilled water was then added to the tube. The liposome suspension (1.0 wt %) was prepared with a tip-type sonicator (Tomy Seiko UR-200P) at 60 W for 10 min under a nitrogen atmosphere. Freshly prepared liposome suspensions were sealed and incubated at 4, 8, or 20 °C to induce liposomal fusion and to analyze the effect of molecular packing in liposomes upon polymerization. AAPD (3.5 mg; 5 mol % to

0024-9297/88/2221-0319$01.50/0